Journal of Atmospheric and Solar-Terrestrial Physics 138-139 (2016) 23–31

Contents lists available at ScienceDirect

Journal of Atmospheric and Solar-Terrestrial Physics

journal homepage: www.elsevier.com/locate/jastp

Research paper

Effect of gravity waves on the tropopause temperature, height and water vapor in Tibet from COSMIC GPS Radio Occultation observations

Attaullah Khan [a,b], Shuanggen Jin [a,c,*]

[a] Key Laboratory of Planetary Sciences, Shanghai Astronomical Observatory, Chinese Academy of Sciences, Shanghai 200030, PR China
[b] University of Chinese Academy of Sciences, Beijing 100049, PR China
[c] Department of Geomatics Engineering, Bulent Ecevit University, Zonguldak 67100, Turkey

ARTICLE INFO

Article history:
Received 24 August 2015
Received in revised form
1 December 2015
Accepted 7 December 2015
Available online 8 December 2015

Keywords:
Tropopause
Gravity wave
GPS Radio Occultation
Tibet

ABSTRACT

The tropopause plays an important role in climate change, particularly in Tibet with complex topography and climate change system. In this paper, the temperature and height of the Cold Point Tropopause (CPT) in Tibet are obtained and investigated from COSMIC (Constellation Observing System for Meteorology, Ionosphere and Climate) GPS Radio Occultation (RO) during June 2006–Feb 2014, which are compared with Lapse Rate Tropopause (LRT) from Atmospheric Infrared Sounder (AIRS/NASA). Furthermore, the impact of Gravity waves (GW) potential energy (E_p) on the CPT-Temperature, CPT-Height, and the variation of stratospheric water vapor with GW E_p variations are presented. Generally the coldest CPT temperature is in June–July–August (JJA) with −76.5 °C, resulting less water vapor into the stratosphere above the cold points. The temperature of the cold point increases up to −69 °C during the winter over the Tibetan Plateau (25–40°N, 70–100°E) that leads to increase in water vapor above the cold points (10 hPa). Mean vertical fluctuations of temperature are calculated as well as the mean gravity wave potential energy E_p for each month from June 2006 to Feb 2014. Monthly E_p is calculated at 5° × 5° grids between 17 km and 24 km in altitude for the Tibetan Plateau. The E_p raises from 1.83 J/Kg to 3.4 J/Kg from summer to winter with mean E_p of 2.5 J/Kg for the year. The results show that the gravity waves affect the CPT temperature and water vapor concentration in the stratosphere. Water vapor, CPT temperature and gravity wave (E_p) have good correlation with each other above the cold points, and water vapor increases with increasing E_p.

1. Introduction

Recently the upper troposphere and lower stratosphere (UTLS) received more attentions because of the important role in climate changes. The tropopause is the separating layer between the troposphere and the stratosphere. The annual cycle in tropopause temperature involves in the penetration of Hadley circulation cell into the lower stratosphere. The tropopause plays a massive role in the stratosphere–troposphere exchange and climate variability to allow/forbid different constituents to the stratosphere (Holton et al., 1995; Gettelman et al., 2011), particularly in Tibet with complex topography and climate change system (Liu and Zhang, 1998; Liu and Chen, 2000). The magnitude of stratospheric water vapor is strongly dependent on the tropopause temperature (TPT) (Rosenlof and Reid, 2008). The global warming study is mainly focused on CO_2 concentration, because water vapor is usually assumed to be balanced by the precipitation due to the short residence time in the troposphere. However the stratosphere water vapor concentration is changing with the time since the residence time of water vapor is longer than one year. Holton et al. (1995) and Mote and Coauthors (1996) showed that a small variation of water vapor (increase or decrease) in the stratosphere can significantly change the climate below by changing the global radiation budget. Therefore the tropopause was paid more attention in the recent epoch (Solomon et al., 2010; Gettelman et al., 2010). Annual cycle of the tropopause temperature and altitude is a significant feature that influences the climatic conditions of the region.

Study on the annual cycle of the tropical tropopause temperature suggests the significant role of vertically propagating Rossby and gravity waves (Garcia, 1987; Gray and Dunkerton, 1990; Haynes et al., 1991; Yulaeva et al., 1994; Holton et al., 1995). The Whole Atmosphere Community Climate Model (WACCM) higher simulation shows that warming effect around the tropopause is caused less by radiative effects, and more by warming effects from dynamical transport or convection (Wang et al., 2013). Theoretical, observational and modeling efforts clarify the sources

* Corresponding author at: Key Laboratory of Planetary Sciences, Shanghai Astronomical Observatory, Chinese Academy of Sciences, Shanghai 200030, PR China.
E-mail addresses: sgjin@shao.ac.cn, sgjin@beun.edu.tr (S. Jin).

http://dx.doi.org/10.1016/j.jastp.2015.12.001
1364-6826/

of gravity waves that are generated by meteorological events, such as typhoon, and convections propagating to the lower and upper stratosphere. De la Torre et al. (2004, 2006) observed important wave activities in the upper troposphere and lower stratosphere at mid-latitudes (30–40°S) above the Andes Range using temperature profiles retrieved from GPS Radio Occultation (GPS RO) between June 2001 and March 2003. Their results suggested that the major sources in this area were topography, jet-stream and convection. It was also illustrated that these sources were continually in action in this area, and different sources could act simultaneously. It should be noted that there are still some limitations and questions for the space-borne remote sensing technique, and the ground based observations and denser space observations are important to depict detailed characteristics of gravity waves in a local region.

Secondary gravity wave is generated by the breakdown of primary gravity wave in the lower stratosphere and transports water vapor to the stratosphere (Lane and Sharman, 2006). Water vapor in the stratosphere resides for a long time, more than one year and the stratospheric water vapor change should be considered as climate forcing not a simple response (Wang et al., 2009). When gravity waves break, it transports energy and momentum to the background and increases energy to the surrounding atmosphere. The role of gravity wave (GW) is very important to keep balance in atmospheric circulations by transporting energy and momentum to different altitudes. Gravity waves are more active in winter than in summer at lower stratosphere. The time and height variation of the wind velocity due to gravity waves showed a clear correlation with high relative humidity, observed by MU (Middle and Upper Atmosphere) radar (Murayama et al., 1994). Gravity wave generated in the troposphere propagates to the middle and upper atmosphere and transfers energy and momentum (Ern et al., 2013). Due to the low density of the air, the amplitude of the GW increases with higher amplitude at high altitude. Potential energy of GW related to the subtropical jet stream with some contribution of regional topography, calculated as mean wintertime E_p, exceeds 2.4 J kg^{-1} above the Himalayas and East China (Alexander et al., 2008). Most of the gravity wave's sources are positioned in the troposphere.

Previous studies showed that gravity waves transport not only energy and moment but also play a critical role in the global circulation and the temperature and constituent structures (i.e. water vapor, ozone concentrations and other chemical constituents) in the atmosphere (Moustaoui et al., 2004; Wang and Alexander, 2010). Therefore, the parameterization of gravity waves needs more improvements and high accuracy observations in wave propagation, amplitude and wavelength. In addition, a high spatial resolution instruments are required for a better study and reliable results, particularly in Tibet with lack of in-situ measurements. Nowadays, COSMIC Radio Occultation observations with six satellites provide unique global high-resolution temperature profiles, which can be used to study the characteristics of the gravity wave in lower atmosphere (e.g., Zeng et al., 2012; Faber et al., 2013; Jin et al., 2014). In this paper, the temperature and height of the Cold Point Tropopause (CPT) in Tibet are obtained and studied from denser COSMIC GPS Radio Occultation observations during June 2006–Feb 2014. Effects of gravity wave's potential energy on the CPT-Temperature, CPT-Height, and stratospheric water vapor are discussed. In Section 2, methods and observation data are introduced, and results are presented in Section 3. Finally conclusions are given in Section 4.

2. Data and methods

2.1. Observation data

The six FORMOSAT-3/COSMIC (Constellation Observing System for Meteorology, Ionosphere & Climate) satellites were launched in April 2006 by Taiwan/USA with final altitude of about 800 km. The orbital inclination of COSMIC satellites is 72°. COSMIC GPS Radio Occultation (RO) provides high resolution observations at Upper Troposphere and Lower Stratosphere (UTLS), which can be used to study the GW potential energy (E_p) in the stratosphere using the temperature profile.

COSMIC GPS RO observations from six satellites provide higher accuracy atmospheric and ionospheric products with up to 1500 to 2000 RO profiles per day. The variation of refractive index n along a GPS RO limb path in the Earth's atmosphere is dominated by the vertical density gradient. Since the refractivity decreases with the altitude generally, a negative sign is added in order to keep a positive bending angle. By inverting the equation through the Abelian transformation, the refractive index n can be written as a function of the bending angle a (Fjeldbo et al., 1971). In the neutral atmosphere, n is conveniently expressed in terms of refractivity defined as $N = (n - 1) \times 10^6$ through the relationship [Kursinski et al., 1997], which is related to the total pressure P and water vapor partial pressure Pw, temperature T, electron number density n_e, signal frequency f and liquid water content W, respectively. Therefore, using COSMIC GPS RO observations, the pressure, temperature and water vapor profiles in the troposphere and electron density profiles in the ionosphere are inversed (e.g., Anthes et al., 2008; Jin et al., 2011; Ho et al., 2010 and 2012; Jin et al., 2014). More information on COSMIC GPS RO products can be found at http://cdaac-www.cosmic.ucar.edu. The COSMIC RO has about 600 occultation per month over the Tibetan plateau (25–40°N, 70–100°E), which provide more atmospheric products over this area. The COSMIC Data Analysis and Archive Center (CDAAC) is responsible for processing the science data received from COSMIC satellites. Staten and Reichler (2008) examined that the COSMIC wet atmospheric temperature profile (wetPrf) has negligible difference with the dry one (atmPrf). In this study, the dry atmospheric temperature profile (atmPrf) is used from http://cdaac-www.cosmic.ucar.edu/cdaac. The temperature data (version 2010.2640) from June 2006 to Feb 2014 are used for the study on tropopause and gravity wave over the Tibetan Plateau.

Reanalysis data of Modern Era Retrospective-Analysis for Research and Applications (MERRA) (http://disc.sci.gsfc.nasa.gov/mdisc) and Atmospheric Infrared Sounder (AIRS) (http://airs.jpl.nasa.gov) are also used for water vapor. The MERRA is a NASA reanalysis using a modern satellite data and the Goddard Earth Observing System Data Assimilation System Version 5 (GEOS-5), which focuses on historical analyses of the hydrological cycle (Rienecker et al., 2011). The AIRS is the first new generation operational remote sensors for upwelling atmospheric emission (Aumann et al., 2003). The AIRS is cross-track-scanning nadir sounders with a swath of ~1650 km wide. More than 2000 channels cover 3.71–4.61, 6.2–8.22, and 8.8–15.4 μm in infrared bands, and therefore the AIRS can sense atmospheric temperature, trace gases, water vapor, and surface temperature with very high accuracies.

2.2. Theory and method

COSMIC GPS radio occultation provides the information of neutral atmospheric parameters from near surface to altitude of 40 km. In this study the temperature profiles are used to observe the GW activities by neglecting the humidity effect (dry temperature profile). This profile is accurate with up to altitude of

10 km in moist troposphere. In order to study the climatology behavior of the GW, the potential energy is calculated using the dry temperature profile retrieved from COSMIC GPS RO (Hei et al., 2008, Tsuda et al., 2000) and potential energy calculated similarly to the method use by Hei et al. (2008).

The total energy of gravity wave is

$$E_0 = E_k + E_p \quad (1)$$

where E_k and E_p are kinetic and potential energy of gravity wave, respectively, while E_0 is the total energy. From the linear theory of the GW the ratio of E_k to E_p is constant and equal to spectral index p ranging from 5/3 to 2.0 (VanZandt, 1985). Obtained data are binned into grid $5^\circ \times 5^\circ$ for each month and mean temperatures ($\bar{T}$) are calculated using the high pass filtering by 1 km vertical average mean, while the monthly mean is calculated for altitude 17–24 km. Temperature perturbation ($\dot{T}$) is obtained by equation ($\dot{T} = T - \bar{T}$), where T is from the COSMIC dry temperature profile and $\bar{T}$ is the background temperature (mean temperature). To avoid edge effect of the height, the half cosine function is applied. From the temperature fluctuation profile, the potential energy is calculated as

$$E_P = \frac{1}{2}(g/N)^2 \overline{(\dot{T}/\bar{T})^2} \quad (2)$$

where g is the gravitational acceleration, N is the Brunt Väisälä frequency. Total energy (E_0) can be calculated from the temperature profile (Tsuda et al., 2000).

The gravity waves potential energy E_p can be use as a proxy for gravity wave activity in the stratosphere. Mean monthly E_p is calculated from June 2006 to Feb 2014, which is used to study the climatology behavior of the gravity wave. The mean E_p value is calculated above the tropopause, because the sharp bending of the temperature variations near the tropopause level creates problem in calculating E_p.

3. Results and analysis

The Tibetan Plateau is very complex in climate change system (Liu and Zhang, 1998; Liu and Chen, 2000; Jin et al., 2013) and also affects the climate change of the region. In this study we aim to show how gravity waves affect the tropopause height and tropopause temperature and analyze gravity wave impact on stratospheric water vapor. Gravity wave plays a critical role in regulating stratospheric water vapor by inducing the mean upwelling or by perturbing the mean temperature structures of the tropopause.

3.1. CPT and LRT temperature (CPT-T and LRT-T)

According to the definition of World Metrological Organization (WMO, 1957), the Lapse Rate Tropopause (LRT) was defined as the level where the temperature lapse rate is less than 2 °C km^{-1} and the average lapse rate between this level and the next 2 km does not exceed 2 °C km^{-1}. The Lapse Rate Tropopause (LRT) temperature and height are calculated from Atmospheric Infrared Sounder (AIRS/NASA). The CPT temperature properties are examined in the Tibetan region using the COSMIC RO temperature profile, which are consistent with previous studies above the LRT.

A number of studies have found that horizontal distribution of CPT temperature and its seasonal cycle are not homogeneous in longitudinal direction. For example, it was observed that CPT was colder in JJA (June–July–August) and warmer in DJF (December–January–February), while the height was anti-correlated with its temperature in the Tibetan Plateau (Feng et al., 2011). The mean temperature variations of CPT and LRT from 2006 to 2014 have the same pattern that the temperatures in DJF are more variable than JJA in the Tibetan plateau. The CPT and LRT temperatures decrease in summer months (JJA). During the summer, the monthly mean temperature of CPT over the Tibetan Plateau reaches its minimum value of −76.5 °C (Fig. 1) and this low temperature of CPT reduces the water vapor to reach the low and middle stratosphere during the JJA months. Water vapor concentration strongly depends on the CPT temperature (Rosenlof and Reid, 2008) since water vapor transportation depends on the thermal characteristics of CPT (Holton et al., 1995; Mote and Coauthors, 1996). While the mean CPT temperature during the winter increases up to −69 °C. So the maximum variation in CPT temperature during the year is around 7° to 8 °C. The mean temperature of LRT reaches −74 °C in

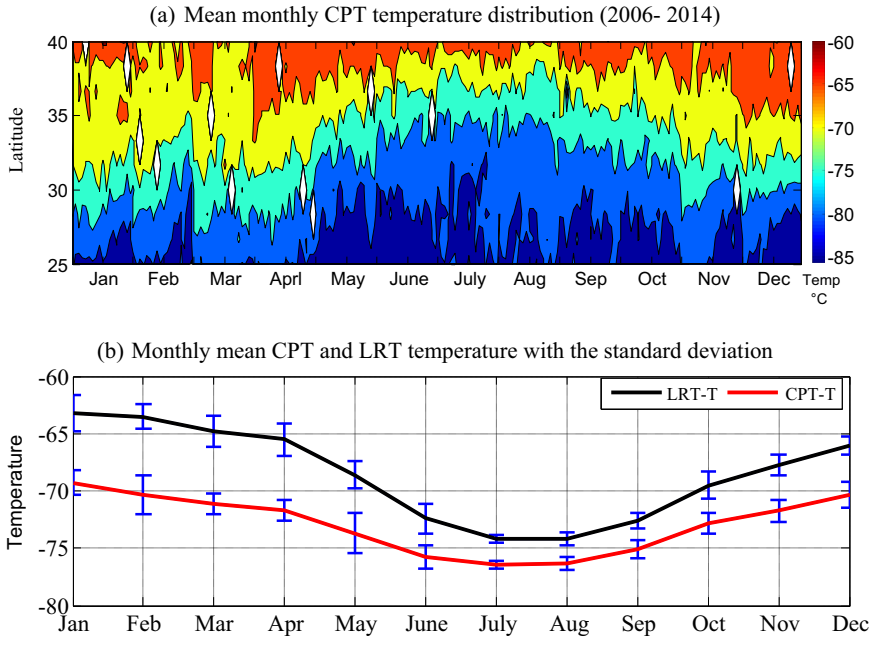

Fig. 1. Seasonal variations of mean monthly Cold Point tropopause (CPT) and Lapse Rate tropopause (LRT) temperatures from 2004 to 2016. (a) Mean monthly CPT temperature distribution (2006–2014) and (b) Monthly mean CPT and LRT temperature with the standard deviation.

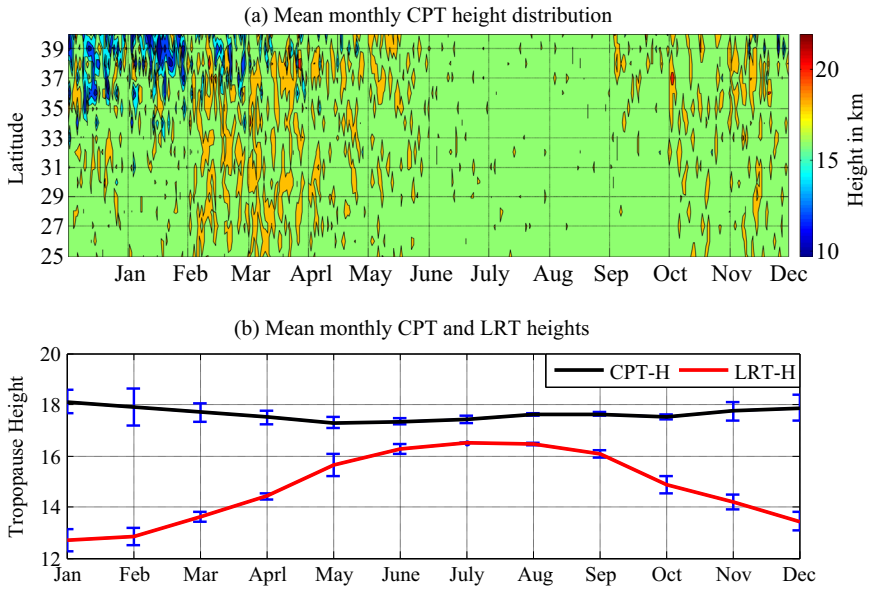

Fig. 2. Seasonal variations of mean monthly Cold Point Tropopause (CPT) and Lapse Rate Tropopause heights from 2006 to 2014. (a) Mean monthly CPT height distribution and (b) Mean monthly CPT and LRT heights.

summer and −64.0 °C in winter, thus total variation in LRT is about 10 °C. The total trend from 2006 to 2014 is 0.90 °C/decade in LRT and 0.61 °C/decade in CPT.

3.2. CPT and LRT height (CPT-H and LRT-H)

Schreiner et al. (2007) found that COSMIC refractivity is about 1% in lower troposphere and 0.2% at 20 km and approaches to 1% at 40 km of height and the temperature accuracy is better than 0.5 k. Temperature profiles with high errors are filtered in this study. Fig. 2(a) and (b) show the Cold Point and Lapse Rate Tropopause heights. The seasonal variations of the LRT height and temperature show anti-correlation, which has a great agreement with earlier studies (Randel et al., 2000; Santer et al., 2003). For the Tibetan region, however, the variation of CPT height and temperature seems to have positive correlation i.e. they are high in the winter and low in the summer. This result is conflicting with Gettelman and de F. Forster (2002), which suggested that the CPT is the lowest during the winter and the highest during the summer in the tropical zone.

The temperature of LRT also decreases during the JJA months but the height of LRT increases and the total seasonal variation in LRT-H is 4 km during the year. For the long time variation from 2006 to 2014, the total trend in LRT-H is decreasing at 495 m per decade, but the height of CPT-H is increasing at 220 m per decade. The trend between CPT and LRT heights is opposite. The height and temperature of LRT are anti-correlated in the Tibetan Plateau, which shows different from the tropical tropopause (Randel et al., 2000; Santer et al., 2003; Schmidt et al., 2008). However, the opposite seasonal variations of the CPT height were verified by Seidel et al. (2001), when they designated the zone of 10°N–10°S as the tropics. This shows that the CPT behaves different seasonal variations with the latitude.

3.3. Influence of gravity wave on CPT-T and CPT-H

In addition, we further investigate the gravity wave impact on CPT and water vapors. The gravity wave plays a main role in regulating CPT temperature. The impact of GW is mostly responsible for the decadal change in the CPT temperature and water vapor in the lower and upper stratosphere. The breaking of these gravity waves in the stratosphere transports not only energy and momentum to the surroundings but also chemical and atmospheric constituents (e.g., Moustaoui et. al., 2004). The gravity wave breaking is responsible for transportation of water vapor across the tropopause and formation of cirrus clouds in lower stratosphere (Wang, 2003). The GW breaking transfers energy to the surroundings and increases the temperature of the surrounding, which affects the CPT temperature (i.e. stratosphere sudden worming).

Mountain generated gravity waves (Mountain waves) impact mesoscale circulations by transporting energy and momentum

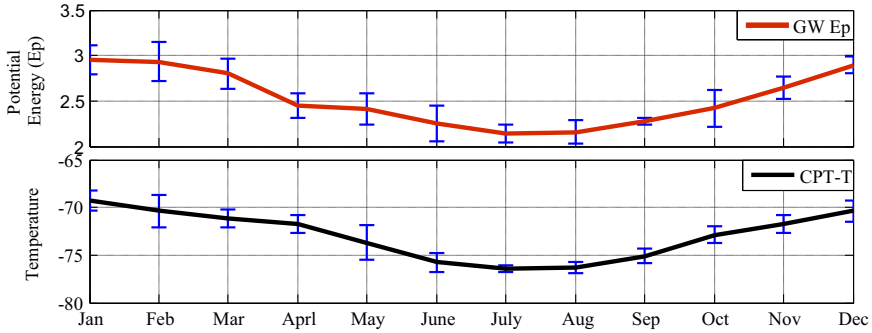

Fig. 3. Relation between CPT temperature (°C) and gravity waves (potential energy E_p) with the standard deviation from 2006 to 2014.

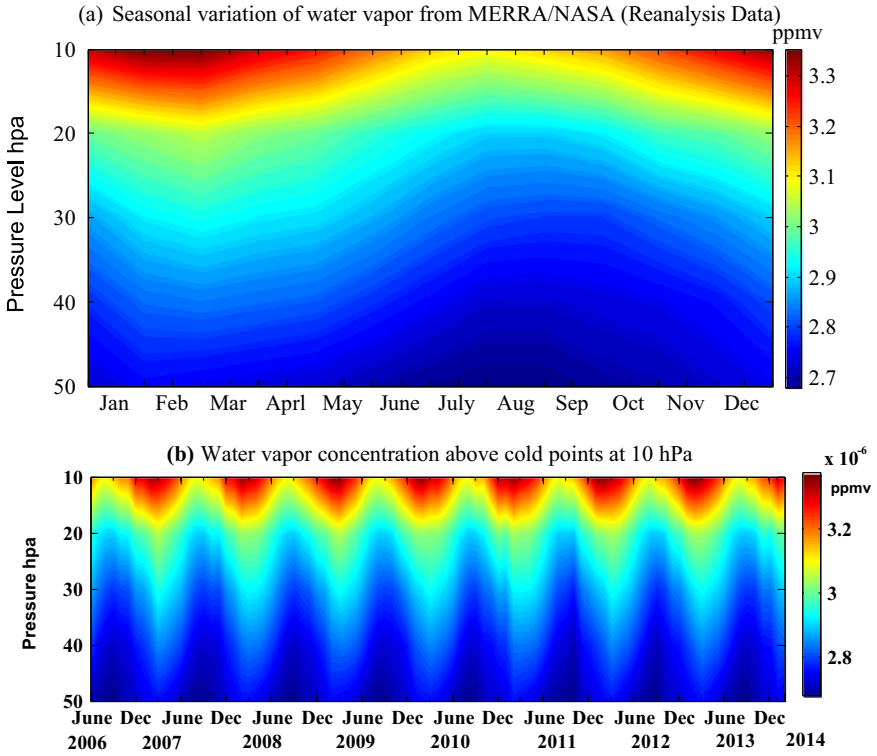

Fig. 4. Water vapor variation above the cold point from MERRA/NASA reanalysis data, MAIMNPANA.5.2.0 (part per million volume, ppmv) during 2006–2014. (a) Seasonal variation of water vapor from MERRA/NASA (Reanalysis Data) and (b) Water vapor concentration above cold points at 10 hPa.

from lower troposphere to the lower and upper stratosphere and maintain the momentum and energy balance (Fritts and Alexander, 2003). It also suggested that the topography, frontal activity, wind shear, jet-stream, convection, and cyclone are the major sources for gravity waves generation. Mountain waves depend on the shape and size of the mountain by the vertical profiles of temperature (T), wind speed and moisture in the impinging flow (Durran, 2003). These gravity waves play an effective role in the atmosphere variation over the Tibetan Plateau. MST radar (Mesosphere, Stratosphere, Troposphere RADAR) observations showed that the tropopause height is modulated by inertia gravity waves at Gadanki, and has the similar features as that of wind components (Das et al., 2010). Randel et al. (2003) examined the tropical CPT and concluded that variations in CPT temperature and height are related to waves like fluctuations such as gravity waves or Kelvin waves, and further observed that large amount of 'wavy' variability in the tropopause region and throughout the stratosphere is related to gravity waves. Gravity waves have an associated energy flux, so departures from conservative propagation will lead to energy dissipation and local heating of the atmosphere (Fritts and Alexander, 2003).

In this work, we calculated the mean gravity wave potential energy from June 2006 to Feb 2014 over the Tibetan Plateau, for the altitude 17–24 km above the tropopause. GW E_p and CPT-T have a good correlation as presented in Fig. 3. The result shows that when GW (E_p) increases in DJF, the temperature of the CPT also increases with the same pattern. These results agree well with previous studies, e.g. Alexander et al. (2008), who calculated the mean Ep exceeds 2.4 J/kg in the Himalayas and Eastern China during the winter. The calculated mean LRT height for the

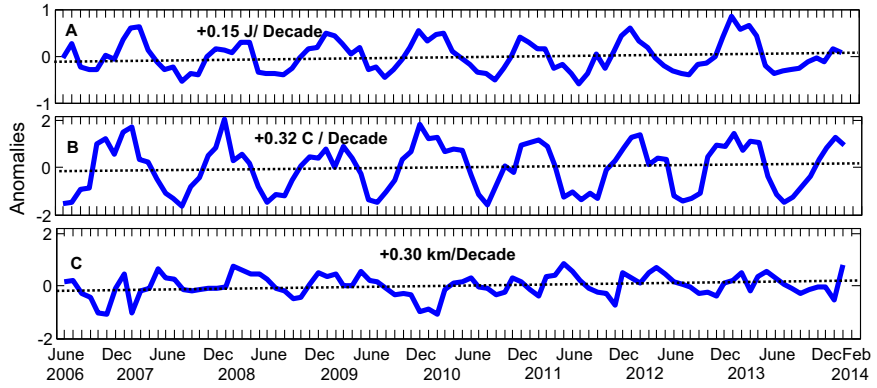

Fig. 5. Time series of mean monthly anomalies in the Tibetan Plateau at (25°N–40°N and 70°E–100°E) for GW potential energy E_p with the trend line (A), CPT temperature (B), and CPT height (C).

tropopause is 14.7 km over the Tibetan Plateau, which increases during JJA season up to 16.5 km and decreases to 12.5 km in DJF. The sharp bending and temperature variations near the tropopause affect the calculations E_p. We select a height of 17 Km to avoid the tropopause effect on gravity waves mean values.

Fig. 3 shows the seasonal cycle of CPT temperature and Ep with a good correlation between the GW (E_p) and CPT temperature. When the potential energy E_p increases, CPT temperature also increases. The seasonal cycle of the gravity waves shows a clear activity in the lower stratosphere, which is higher in winter and lower in summer and these large E_p affects the temperature structure near the tropopause. The observation shows that gravity waves activity is also high in winter time at middle and high latitudes (Alexander, 1998). Lidar observations also showed the same cycle for gravity waves (e.g.,Whiteway and Carswell, 1995). Gravity waves follow the same behavior in the Tibetan Plateau, smaller as 1.83 J Kg^{-1} in the JJA months (summer season) and higher as 2.70 J Kg^{-1} in winter season.

From June 2006 to February 2014, monthly mean values show that the mean monthly E_p and CPT temperatures (over the Tibetan plateau) have a similar pattern with maxima during the winter and minima during the summer (Fig. 3). This is clear from both patterns that E_p plays a major role in the CPT temperature variation in Tibet area. CPT-H has no clear relation with E_p variation, however, a small variation is not discussed in this work (Fig. 2).

3.4. Gravity wave E_p and water vapor above the CPT

Recent atmospheric variations and global warming are associated with increase in greenhouse gas, while water vapor is one of the most important in greenhouse gases. These gases are responsible for the warming effect on the Earth's surface. Gravity wave is one of the main sources, which diffuses these gases into the stratosphere and upper atmosphere. It is evident from the previous studies that when gravity waves propagate from the troposphere to the stratosphere it transports water vapor and other atmospheric constituents (Wang, 2003; Todd and Sharman, 2006).

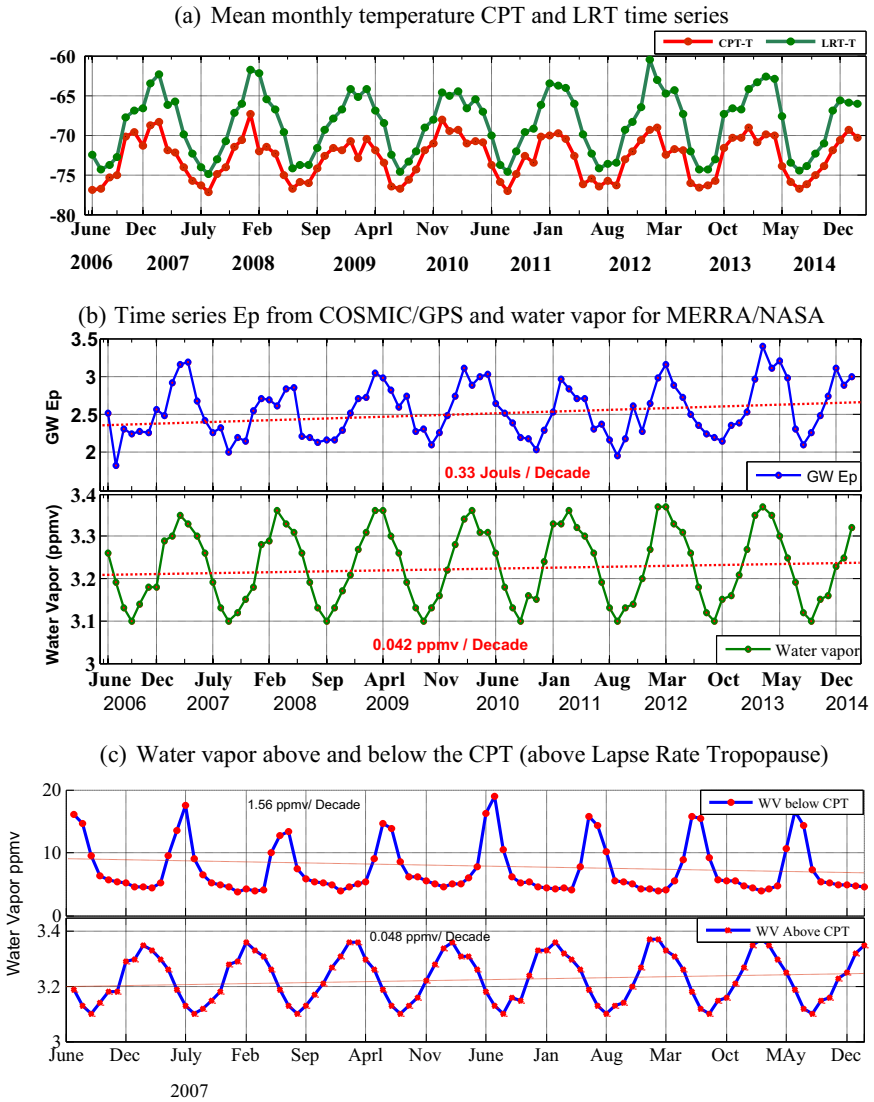

Fig. 6. Time series of mean CPT and LRT temperatures, E_p and water vapor from 2006 to 2014. (a) Mean CPT and LRT temperatures (COSMIC RO), (b) Mean E_p from COSMIC RO and water vapor from MERRA/NASA data, and (c) Water vapor above and below CPT.

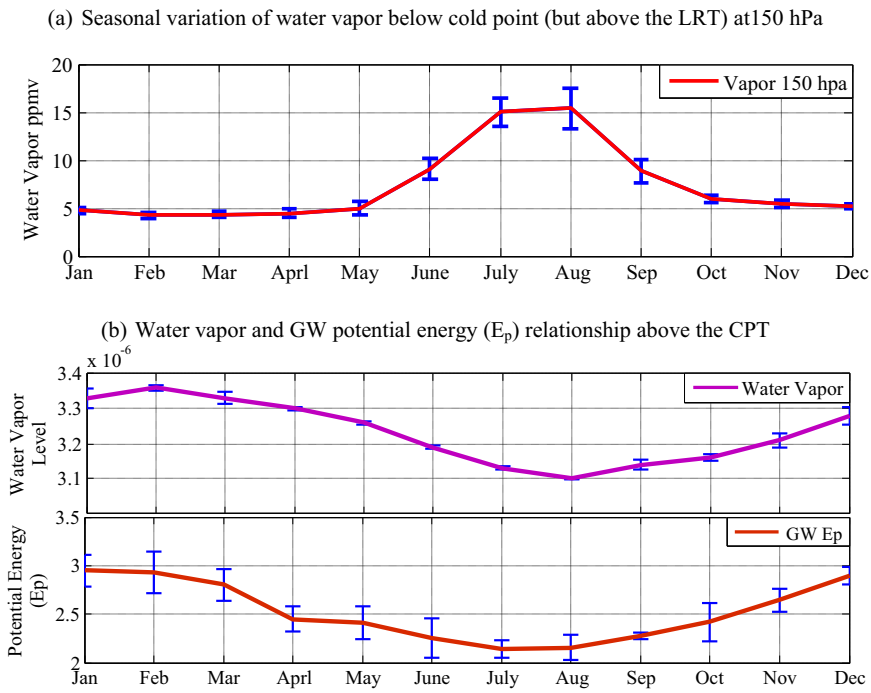

Fig. 7. Mean water vapor concentration below the cold point (but above the LRT) at150 hPa with the standard deviation in each month (a), and mean water vapor at 10 hPa above the cold points and mean E_p with the standard deviation in each month (b).

Here the reanalysis product MAIMNPANA.5.2.0 of water vapor averaged over longitude 70°E–100°E and latitude 25°N–40°N from MERRA/NASA is compared with E_p from COSMIC GPS RO. The result shows a good correlation above the cold point. The water vapor increases in DJF above the CPT and decreases in the Monsoon season in JJA. MERRA/NASA reanalysis data show that the humidity decreases in JJA and enhances in DJF (Fig. 4). The trend in the gravity wave increases by 0.15 J decade^{-1} in Fig. 5 and in the water vapor also increases in Fig. 4 as well as in CPT temperature (Fig. 6a). The increase rate of water vapor in the Tibetan Plateau is 0.04 ppmv decade^{-1}. The increase of water vapor in the stratosphere is small but its impact is large in the area. The trends show that the GW activities are increasing in the Tibetan Plateau as shown in Fig. 5.

We use the MERRA water vapor reanalysis data for two different altitudes, 150 hPa and 10 hPa, i.e. below the cold point and above the cold points (Fig. 6c). The results show that below CPT (but above LRT) the concentration of water vapor increases during JJA months but above the cold points the concentration increases during the winter seasons when GW (potential energy) is maximum. It shows that water vapor cannot cross the CPT without GW and CPT temperature increase and GW transports water vapors above the cold points. Reanalysis data show that the trend of water vapor decreases below the cold points while increases above the cold points as shown in Fig. 6. We can conclude from these results that gravity waves play a massive role in the water vapor transportation above the cold points (Figs. 4b, 6b and Fig. 7b).

Fig. 8 shows that Ep increases in December–January–February (DJF), and decreases in June–July–August (JJA), which is the same with water vapor in Figs. 4b and 6b. Stratosphere water vapor increases due to the warming of CPT and as a response climate changes occur during the winter season when gravity waves activity increases. MERRA/NASA reanalysis data show that water vapor above the cold point increases only in winter seasons (Fig. 4b and 6b), which may affect the surface temperature due to greenhouse phenomenon. Recently Zhang et al. (2014) confirmed that Lakes temperature increases in the Tibetan Plateau at average rate of 0.012 ± 0.033 °C yr^{-1} (Greenhouse effects). The surface temperature at the east-west Tibetan Plateau shows an increasing trend, especially in winter at about 0.21 °C decade^{-1} for eastern and 0.09 °C decade^{-1} for western region (You et al., 2012). Because greenhouse gases affect the surface temperature and water vapor is one of the greenhouse gas, surface temperature is connected with water vapor.

4. Summary and discussion

The temperatures and heights of CPT and LRT in Tibet are obtained from COSMIC GPS Radio Occultation and AIRS during 2006-2014, respectively. The CPT and LRT temperatures decrease in summer and increase in winter season. The mean temperature of the CPT is −73 °C for the Tibetan Plateau, but reaches the maximum of −69 °C in boreal winter and the minimum of −77 °C in boreal summer. The CPT temperature changes are 7–8 °C during the year. This large difference of the CPT temperature in the year shows the high sensitivity of the Tibetan region to the climate changes. In addition, The CPT is higher and warmer in the winter season, and lower and colder in the summer season. The variability in the CPT and LRT composition is due to a wide spectrum of waves, such as gravity waves. In the region the E_p shows clear variations, decreasing in summer and increasing in winter.

COSMIC GPS RO provides unique observations to study gravity waves in the Tibetan Plateau. The high temperature on the Tibetan plateau (TP) surface triggers deep convective mixing in the lower troposphere. The calculated E_p, CPT temperature and water vapor from the MERRA/NASA shows good correlation. The gravity waves activities are enhanced during the winter season over the Tibetan Plateau that lead to increase the CPT temperature and alow water vapor to defuse into the stratosphere. When gravity waves propagate and break, it transports not only energy and momentum, but also deposits vertical mixing of heat and affects CPT temperature directly or indirectly. Defusing water vapor and trace gases to the stratosphere, as a result concentration of water vapor above the cold point increases. This increase may affect the Tibetan Plateau climate system and change the surface temperature

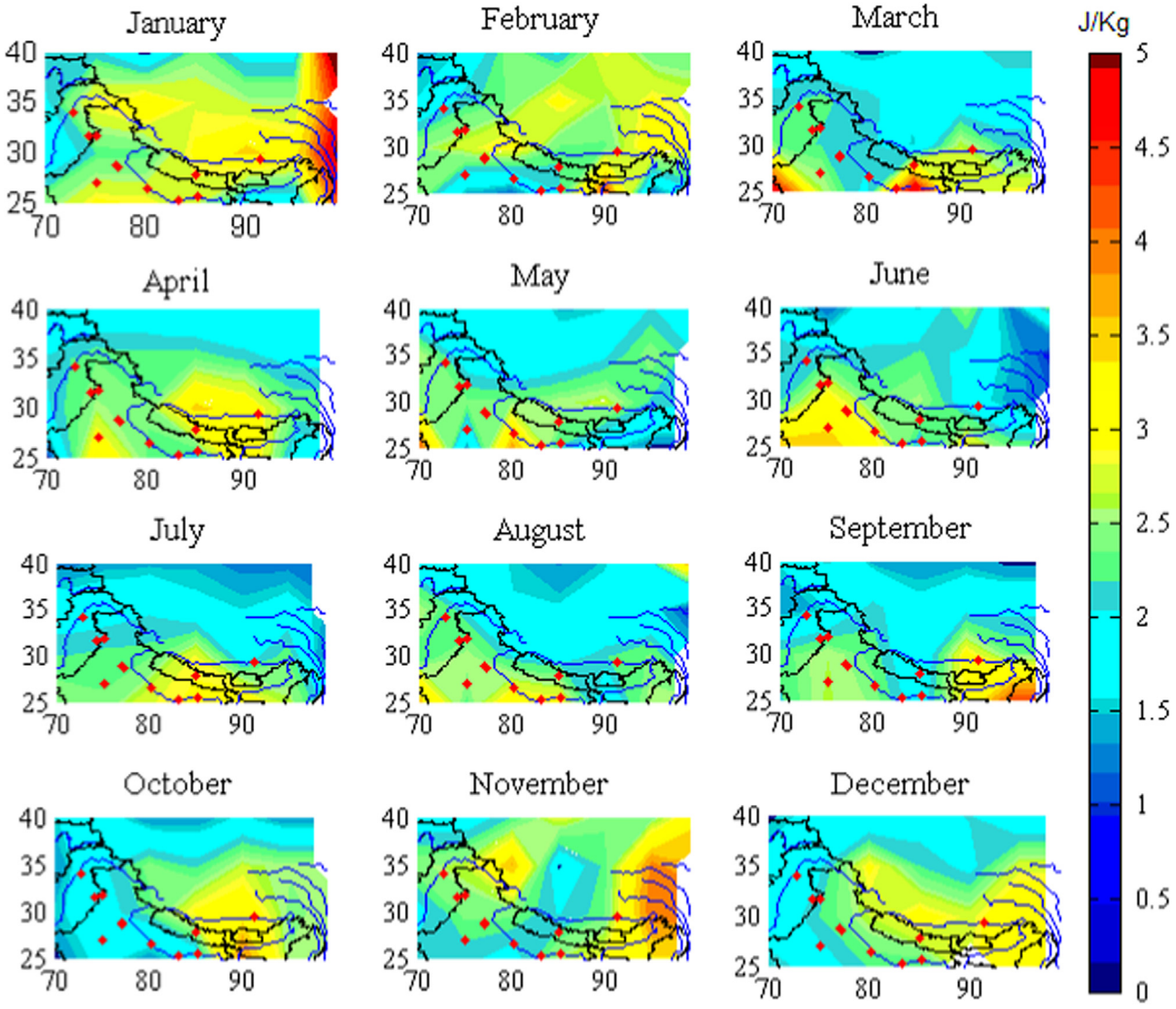

Fig. 8. Monthly mean potential energy (E_p) distribution at altitude 17–24 km over the Tibetan Plateau by average $5^\circ \times 5^\circ$, where the red dot shows main cities. (For interpretation of the references to color in this figure legend, the reader is referred to the web version of this article.)

(Green house effect) while GW plays a main role.

Gravity wave is the source that transports the water vapor from low altitudes to high altitudes. Warming over the Tibetan Plateau is caused by the greenhouse gases diffusion in the stratosphere, which may have larger effects than the rest of the world (Duan et al., 2006). The surface temperature in the east-west Tibetan Plateau shows a warming trend, especially in winter, and further study is required in the future.

Acknowledgments

This work was supported by the Shanghai Science and Technology Commission Project (Grant No. 12DZ2273300), and National Natural Science Foundation of China (NSFC) Project (Grant Nos. 11373059 and 11573052). Great appreciation is extended to the CDAAC for providing the COSMIC GPS RO data.

References

Anthes, R.A., Bernhardt, P.A., Chen, Y., et al., 2008. The COSMIC/FORMOSAT-3 mission: early results. Bull. Am. Meteorol. Soc. 89, 313–333.

Alexander, S.P., Tsuda, T., Kawatani, Y., 2008. COSMIC GPS observations of northern hemisphere winter stratospheric gravity waves and comparisons with an atmospheric general circulation model. Geophys. Res. Lett. 35, L10808. http://dx.doi.org/10.1029/2008GL033174.

Alexander, M.J., 1998. Interpretations of observed climatological patterns in stratospheric gravity wave variance. J. Geophys. Res. 103 (D8), 8627–8640.

Aumann, H., Chahine, M.T., Gautier, C., et al., 2003. AIRS/AMSU/HSB on the Aqua mission: design, science objectives, data products, and processing systems. IEEE Trans. Geosci. Remote Sens. 41, 253–264. http://dx.doi.org/10.1109/TGRS.2002.808356.

Das, S.S., Kumar, K.K., Uma, K., 2010. MST radar investigation on inertia-gravity waves associated with tropical depression in the upper troposphere and lower stratosphere over Gadanki (13.51N, 79.21E). J. Atmos. Terr. Phys. 72, 1184–1194.

De la Torre, A., Tsuda, T., Hajj, G., Wickert, J., 2004. A global distribution of the strato- spheric gravity wave activity from GPS occultation profiles with SAC-C and CHAMP. J. Meteorol. Soc. Jpn. 82, 407–417.

De la Torre, A., Alexander, P., Llamedo, P., Menendez, C., Schmidt, T., Wickert, J., 2006. Gravity waves above the Andes detected from GPS radio occultation temperature profiles: jet mechanism? Geophys. Res. Lett. 33, L24810. http://dx.doi.org/10.1029/ 2006GL027343.

Duan, A.M., Wu, G., Zhang, Q., Liu, Y., 2006. New proofs of the recent climate warming over the Tibetan Plateau as a result of the increasing greenhouse gases emissions. Chin. Sci. Bull. 51, 1396–1400.

Durran, D.R., 2003. Lee waves and mountain waves. Encycl. Atmos. Sci., 1161–1169.

Ern, M., Aaras, C., Faber, A., Ffohlich, K., Jacobi, C., Kalisch, S., Krebsbach, M., Preusse, P., Schmidt, T., Wickert, J., 2013. Observations and Ray Tracing of Gravity Waves: Implications for Global Modeling, Climate and Weather of the Sun-Earth System (CAWSES). Springer Atmospheric Sciences, Netherlands, 10.1007/978-94-007-4348-9-21.

Faber, A., Llamedo, P., Schmidt, T., de la Torre, A., Wickert, J., 2013. On the

determination of gravity wave momentum flux from GPS radio occultation data. Atmos. Meas. Tech. 6 (2013), 31693180.
Feng, S., Fu, Y., Xiao, Q., 2011. Is the tropopause higher over the Tibetan Plateau? Observational evidence from Constellation Observing System for Meteorology, Ionosphere, and Climate (COSMIC) data. J. Geophys. Res. 116, D21121. http://dx.doi.org/10.1029/2011JD016140.
Fjeldbo, G., Kliore, A.J., Eshleman, V.R., 1971. The neutral atmosphere of Venus as studied with the Mariner V radio occultation experiment. Astron. J. 76, 123–140. http://dx.doi.org/10.1086/111096.
Fritts, D.C., Alexander, M.J., 2003. Gravity wave dynamics and effects in the middle atmosphere. Rev. Geophys. 41 (1), 1003. http://dx.doi.org/10.1029/2001RG000106.
Garcia, R.R., 1987. On the mean meridional circulation of the middle atmosphere. J. Atmos. Sci. 44, 3599–3609.
Gettelman, A., Hegglin, M.I., Son, S.W., et al., 2010. Multimodel assessment of the upper troposphere and lower stratosphere: Tropics and global trends. J. Geophys. Res. 115, D00M08. http://dx.doi.org/10.1029/2009JD013638.
Gettelman, A., Hoor, P., Pan, L.L., Randel, W.J., Hegglin, M.I., Birner, T., 2011. The extratropical upper troposphere and lower stratosphere. Rev. Geophys. 49, RG3003. http://dx.doi.org/10.1029/2011RG000355.
Gettelman, A., de F. Forster, P.M., 2002. A climatology of the tropical tropopause layer. J. Meteorol. Soc. Jpn. 80 (4B), 911–924.
Gray, L.J., Dunkerton, T.J., 1990. The role of the seasonal cycle in the quasibiennial oscillation of ozone. J. Atmos. Sci. 47, 2429–2451.
Hei, H., Tsuda, T., Hirooka, T., 2008. Characteristics of atmospheric gravity wave activity in the polar regions revealed by GPS radio occultation data with CHAMP. J. Geophys. Res. 113, D04107. http://dx.doi.org/10.1029/2007JD008938.
Haynes, P.H., Marks, C.J., McIntyre, M.E., Shepherd, T.G., Shine, K.P., 1991. On the "Downward Control" of extratropical diabatic circulations by eddy induced mean zonal forces. J. Atmos. Sci. 48, 651–678.
Holton, J.R., Haynes, P.H., McIntyre, M.E., Douglass, A.R., Rood, R.B., Pfister, L., 1995. Stratosphere–troposphere exchange. Rev. Geophys. 33, 403–439.
Ho, S.-P., Zhou, X., Kuo, Y., Hunt, D., Wang, J., 2010. Global comparisons of the radiosonde water vapor measurements in the troposphere using GPS radio occultation from COSMIC. Remote Sens. 2 (5), 1320–1330.
Ho, S.-P., Hunt, D., Steiner, A.K., et al., 2012. Reproducibility of GPS radio occultation data for climate monitoring: Profile-to-profile inter-comparison of CHAMP climate records 2002 to 2008 from six data centers. J. Geophys. Res. 117, D18111. http://dx.doi.org/10.1029/2012JD017665.
Jin, S.G., Cardellach, E., Xie, F., 2014. GNSS Remote Sensing: Theory, Methods and Applications. Springer, Netherlands, p. 276.
Jin, S.G., Feng, G.P., Gleason, S., 2011. Remote sensing using GNSS signals: current status and future directions. Adv. Space Res. 47 (10), 1645–1653. http://dx.doi.org/10.1016/j.asr.2011.01.036.
Jin, S.G., van Dam, T., Wdowinski, S., 2013. Observing and understanding the Earth system variations from space geodesy. J. Geodyn. 72, 1–10. http://dx.doi.org/10.1016/j.jog.2013.08.001.
Kursinski, E.R., Hajj, G.A, Schofield, J.T., Linfield, R.P., Hardy, K.R., 1997. Observing Earth's atmosphere with radio occultation measurements using the Global Positioning System. J. Geophys. Res. 102 (D19), 23429–23465. http://dx.doi.org/10.1029/97JD01569.
Lane, T.P., Sharman, R.D., 2006. Gravity wave breaking, secondary wave generation, and mixing above deep convection in a three-dimensional cloud model. Geophys. Res. Lett. 33, L23813. http://dx.doi.org/10.1029/2006GL027988.
Liu, X., Chen, B., 2000. Climatic warming in the Tibetan Plateau during recent decades. Int. J. Clim. 20, 1729–1742, doi:10.1002/1097- 0088(20001130)20:143.0.CO;2-Y.
Liu, X., Zhang, M., 1998. Contemporary climatic change over the Qinghai Xizang Plateau and its response to the greenhouse effect. Chin. Geogr. Sci. 8, 289–298. http://dx.doi.org/10.1007/s11769-997-0034-9.
Mote, P.W., Coauthors, 1996. An atmospheric tape recorder: The imprint of tropical tropopause temperatures on stratospheric water vapor. J. Geophys. Res. 101D, 3989–4006.
Moustaoui, M., Joseph, B., Teitelbaum, H., 2004. Mixing layer formation near the tropopause due to gravity wave-critical level interactions in a cloud-resolving model. J. Atmos. Sci. 61, 3112–3124.
Murayama, Y., Tsuda, T., Fukao, S., 1994. Seasonal variation of gravity wave activity in the lower atmosphere observed with the MU radar. J. Geophys. Res. 99 (D11), 23057–23069. http://dx.doi.org/10.1029/94JD01717.
Randel, W.J., Wu, F., Gaffen, D.J., 2000. Interannual variability of the tropical tropopause derived from radiosonde data and NCEP reanalyses. J. Geophys. Res. 105, 15,509–15,524.
Randel, W.J., Wu, F., Rivera Ríos, W., 2003. Thermal variability of the tropical tropopause region derived from GPS/MET observations. J. Geophys. Res. 108 (D1), 4024. http://dx.doi.org/10.1029/2002JD002595.
Rienecker, M.M., Suarez, M.J., Gelaro, R., et al., 2011. MERRA: NASA's Modern-Era Retrospective Analysis for Research and Applications. J. Clim. **24**, 3624–3648, doi:10.1175/JCLI-d-11-00015.1.
Rosenlof, K.H., Reid, G.C., 2008. Trends in the temperature and water vapor content of the tropical lower stratosphere: Sea surface connection. J. Geophys. Res. 113, D06107. http://dx.doi.org/10.1029/ 2007JD009109.
Santer, B.D., Sausen, R., Wigley, T., et al., 2003. Behavior of tropopause height and atmospheric temperature in models, reanalyses, and observations: Decadal changes. J. Geophys. Res. 108 (D1), 4002. http://dx.doi.org/10.1029/2002JD002258.
Schreiner, W., Rocken, C., Sokolovskiy, S., Syndergaard, S., Hunt, D., 2007. Estimates of the precision of GPS radio occultations from the COSMIC/FORMOSAT-3 mission. Geophys. Res. Lett. 34, L04808. http://dx.doi.org/10.1029/2006GL027557.
Schmidt, T., de la Torre, A., Wickert, J., 2008. Global gravity wave activity in the tropopause region from CHAMP radio occultation data. Geophys. Res. Lett. 35, L16807. http://dx.doi.org/10.1029/2008GL034986.
Seidel, D.J., Ross, R.J., Angell, J.K., Reid, G.C., 2001. Climatological characteristics of the tropical tropopause as revealed by radiosondes. J. Geophys. Res. 106, 7857–7878. http://dx.doi.org/10.1029/2000JD900837.
Solomon, S., Rosenlof, K.H., Portmann, R.W., Daniel, J.S., Davis, S.M., Sanford, T.J., Plattner, G.-K., 2010. Contributions of stratospheric water vapor to decadal changes in the rate of global warming. Science 327, 1219–1223. http://dx.doi.org/10.1126/science.1182488.
Staten, P.W., Reichler, T., 2008. Use of radio occultation for long-term tropopause studies: uncertainties, biases, and instabilities. J. Geophys. Res. 113, D00B05. http://dx.doi.org/10.1029/2008JD009886.
Tsuda, T., Nishida, M., Rocken, C., Ware, R.H., 2000. A global morphology of gravity wave activity in the stratosphere revealed by the GPS Occultation Data (GPS/MET). J. Geophys. Res. 105 (D6), 7257–7273. http://dx.doi.org/10.1029/1999JD901005.
Todd, P.L., Sharman, R.D., 2006. Gravity wave breaking, secondary wave generation, and mixing above deep convection in a three-dimensional cloud model. Geophys. Res. Lett. 33, L23813. http://dx.doi.org/10.1029/2006GL027988.
VanZandt, T.E., 1985. A model for gravity wave spectra observed by Doppler sounding systems. Radio Sci. 20 (6), 1323–1330. http://dx.doi.org/10.1029/RS020i006p01323.
Wang, P.K., 2003. Moisture plumes above thunderstorm anvils and their contributions to cross-tropopause transport of water vapor in midlatitudes. J. Geophys. Res. 108 (D6), 4194. http://dx.doi.org/10.1029/ 2002 JD002581.
Wang, W., Matthes, K., Schmidt, T., Neef, L., 2013. Recent variability of the tropical tropopause inversion layer. Geophys. Res. Lett. 40, 6308–6313.
Wang, L., Alexander, M.J., 2010. Global estimates of gravity wave parameters from GPS radio occultation temperature data. J. Geophys. Res. 115, D21122. http://dx.doi.org/10.1029/2010JD013860.
Wang, P.K., Setvák, M., Lyons, W., Schmid, W., Lin, Hsin-Mu, 2009. Further evidences of deep convective vertical transport of water vapor through the tropopause. Atmos. Res. 94, 400–408.
Whiteway, J.A., Carswell, A.I., 1995. Lidar observations of gravity wave activity in the upper stratosphere over Toronto. J. Geophys. Res. 100, 14,113–14,124.
You, Q., Fraedrich, K., Ren, G., Pepin, N., Kang, S., 2012. Variability of temperature in the Tibetan Plateau based on homogenized surface stations and reanalysis data. Int. J. Clim. 33, 1337–1347. http://dx.doi.org/10.1002/joc.3512.
Yulaeva, E., Holton, J., Wallace, J., 1994. On the cause of the annual cycle in tropical lower- stratospheric temperatures. J. Atmos. Sci. 51, 169–174.
Zhang, G., Yao, T., Xie, H., Qin, J., Ye, Q., Dai, Y., Guo, R., 2014. Estimating surface temperature changes of lakes in the Tibetan Plateau using MODIS LST data. J. Geophys. Res. Atmos. 119, 8552–8567. http://dx.doi.org/10.1002/2014JD021615.
Zeng, Z., Ho, S.-P., Sokolovskiy, S., Kuo, Y.-H., 2012. Structural evolution of the Madden-Julian Oscillation from COSMIC radio occultation data. J. Geophys. Res. 117, D22108. http://dx.doi.org/10.1029/2012JD017685.